Journal of Computational Physics 547 (2026) 114555

Contents lists available at ScienceDirect

Journal of Computational Physics

journal homepage: www.elsevier.com/locate/jcp

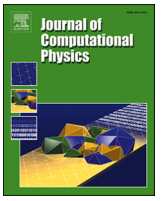

Short note

Interface normal and curvature calculation for the conservative level set method

William Doherty [a,b], Timothy N. Phillips [b], Markus Uhlmann [c], Zhihua Xie [a,c,*]

[a] School of Engineering, Cardiff University, Queen's Buildings, Cardiff, CF24 3AA, United Kingdom
[b] School of Mathematics, Cardiff University, Abacws, Cardiff, CF24 4AG, United Kingdom
[c] Institute for Water and Environment, Karlsruhe Institute of Technology, Karlsruhe, 76131, Germany

ARTICLE INFO

Keywords:
Conservative level set method
Multiphase flows
Surface tension
Curvature
Interface normal
Viscoelastic fluids

ABSTRACT

We proposed a novel diffused interface approach for the interface normal and curvature calculation in the conservative level set method framework for both Newtonian and non-Newtonian multiphase flows. The standard benchmark of reversible vortex problem is used to test the interface capturing method for both standard and conservative level set method. In addition, the new approach is validated to accurately simulate oscillating droplet, bubble rising in a viscoelastic fluid, and droplet impact in a deep pool, in which a good agreement is obtained with analytical solutions and experimental measurements.

1. Introduction

The calculation of normal and curvature is a crucial component of interface capturing techniques for multiphase flows. The nature of the interface contributes to the stability and accuracy of these calculations in that interfaces that are either too sharp or too diffuse often result in poor approximations to the normal and curvature. The standard level set method [1] is easy for normal and curvature calculation, but it might have issues for the mass conservation and diffused profile. The conservative level set method (CLSM) [2] is good for mass conservation and capturing sharp interface, but suffers from poor normal and curvature calculations, which is crucial for some surface tension dominant flows. In this short note, we propose a new approach to bridge the two level-set methods and compare different approaches for performing these calculations for the CLSM.

The diffused interface approach was introduced to stabilise the calculation of the curvature for the volume-of-fluid (VOF) method on unstructured meshes [3]. This should not be confused with the diffuse-interface method [4] for interface capturing which is a more general multiphase representation technique. When volume fraction is used to calculate the normal to the interface, the VOF method experiences similar stability issues as those associated with the conservative level-set function.

In conventional VOF methods an approach based on a height function has been used to determine the curvature which circumvents this issue [5]. However, the reconstruction of the height function on unstructured meshes is non-trivial. This motivated Xie et al. [3] to develop the diffused interface approach which employs a diffused volume fraction solely for the purpose of calculating the interface curvature. The aim of this short note is to extend this approach for the CLSM framework using a finite element method with triangular meshes (detailed numerical method can be found in [6]) and compare with the original [2] and other stabilised [7] CLSMs.

* Corresponding author.
E-mail address: zxie@cardiff.ac.uk (Z. Xie).

https://doi.org/10.1016/j.jcp.2025.114555
Received 19 July 2024; Received in revised form 21 November 2025; Accepted 27 November 2025
Available online 30 November 2025

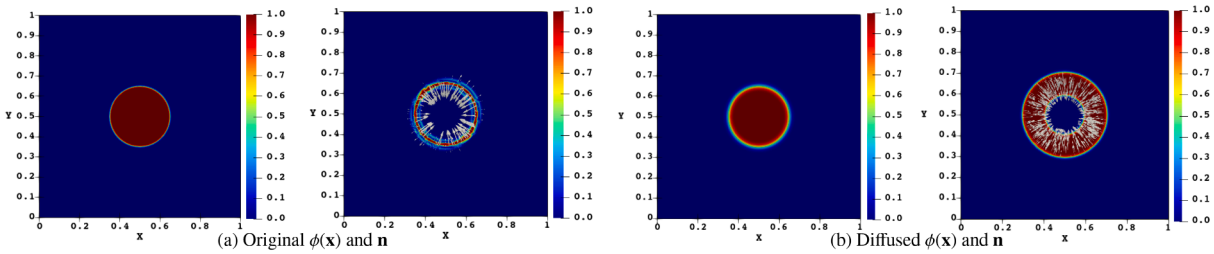

Fig. 1. Comparison of original and the diffused interface approach on the conservative level-set function: (a) initial $\phi(x)$ and its L^2 projection of $\mathbf{n}$; (b) diffused $\phi(x)$ and its L^2 projection of $\mathbf{n}$. Here $h = 1/100$, $D = h$, $\Delta\tau = 0.1h$ with 12 iterations performed.

2. Diffused interface approach

The continuity and momentum equations for multiphase flows are

$$\begin{aligned} \nabla \cdot \mathbf{u} &= 0 \\ \rho\left(\frac{\partial \mathbf{u}}{\partial t} + (\mathbf{u}\cdot\nabla)\mathbf{u}\right) &= \nabla\cdot\boldsymbol{\sigma} + \mathbf{F} \end{aligned} \tag{1}$$

where $\mathbf{u}$ is the velocity vector for 2D Cartesian [8] or 3D axisymmetric [6] flows, ρ is the density and $\mathbf{F}$ is a body force including gravity and surface tension. In these equations $\boldsymbol{\sigma}$ is the Cauchy stress tensor defined by:

$$\boldsymbol{\sigma} = -p\mathbf{I} + 2\eta_s\mathbf{D}(\mathbf{u}) + \boldsymbol{\tau}_p \tag{2}$$

where p is the pressure, η_s is the solvent viscosity ($\eta_s = \mu$ for Newtonian fluids), $\mathbf{D}(\mathbf{u}) = \frac{1}{2}\left(\nabla\mathbf{u} + \nabla\mathbf{u}^T\right)$ is the rate-of-strain tensor and $\boldsymbol{\tau}_p$ is the polymeric stress tensor ($\boldsymbol{\tau}_p = \mathbf{0}$ for Newtonian fluids). For viscoelastic fluids the evolution of $\boldsymbol{\tau}_p$ is dictated by a constitutive equation, detailed more in [6].

The conservative level-set function $\phi(\mathbf{x}) = \frac{1}{1+e^{\hat{\phi}(\mathbf{x})/\epsilon}}$ is defined over the domain as a continuous Heaviside function, where $\hat{\phi}$ is a signed distance function and ϵ is a measure of interface thickness. The material parameters of individual phases can be obtained as: $\rho(\phi) = \rho_2\phi + \rho_1(1-\phi), \eta_s(\phi) = \eta_{s,2}\phi + \eta_{s,1}(1-\phi)$. Then we use the conservative level-set method to capture the interface by solving the following advection equation

$$\frac{\partial\phi}{\partial t} + \mathbf{u}\cdot\nabla\phi = 0 \tag{3}$$

and reinitialise the profile of the conservative level-set function using

$$\frac{\partial\phi}{\partial\tau} + \nabla\cdot(\phi(1-\phi)\mathbf{n}) = \epsilon\nabla\cdot(\nabla\phi) \tag{4}$$

where $\mathbf{n} = \frac{\nabla\phi}{|\nabla\phi|}$ is the normal to the level-set function at the continuous level and τ is an artificial time.

In the new diffused interface approach, an additional diffusion equation for the conservative level-set function ϕ

$$\frac{\partial\phi}{\partial\tau} = D\nabla^2\phi \tag{5}$$

is solved over a small number of time steps, where D is the diffusion coefficient and τ is pseudo-time, both chosen according to the amount of diffusion required. The solution to Eq. (5) is used to find the normal vector for the reinitialisation equation via an L^2 projection. It is important to emphasise that the diffused level-set function obtained by solving Eq. (5) is only used for the normal and curvature calculations and not to capture the interface since to do so would compromise the interface location if D is large. The method is only used to simplify the calculation of the normal vector $\mathbf{n}$ for level-set functions with sharp interfaces. The normal vector calculated in this way is also used to calculate the curvature κ for use in the surface tension term. An inaccurate curvature can also contribute to a loss of accuracy and convergence in numerical schemes.

Fig. 1 illustrates the diffused interface approach using a simple example. Consider the two-phase arrangement shown in Fig. 1(a) in which the initial conservative level-set function and the L^2 projection of $\mathbf{n}$ are displayed. Fig. 1(b) displays the level-set function following the solution of Eq. (5) over 12 pseudo-time steps with $\Delta\tau = 0.1h$ and $D = h$ and the corresponding L^2 projection of $\mathbf{n}$. The diffused interface allows for a much more stable L^2 projection of the level-set function to be performed to calculate the normal vector. A small amount of diffusion circumvents the difficulties associated with the normal calculation.

Fig. 2 shows how the diffused interface approach performs when approximating the curvature of an ellipse. In Fig. 2(a) the ellipse, defined by the equation $(x/a)^2 + (y/b)^2 = 1$ with $a = 0.25$ and $b = 0.2$, is shown. The analytical expression for the curvature is $\kappa = -\frac{ab}{(a^2\sin^2\theta + b^2\cos^2\theta)^{3/2}}$ [9] and in Fig. 2(b) this is displayed as a function of θ, the angle shown in Fig. 2(a). The relative error of the curvature κ_d for the undiffused and diffused methods is shown in Fig. 2(c) where it can be seen that both methods predict errors of the order of 10^{-2}.

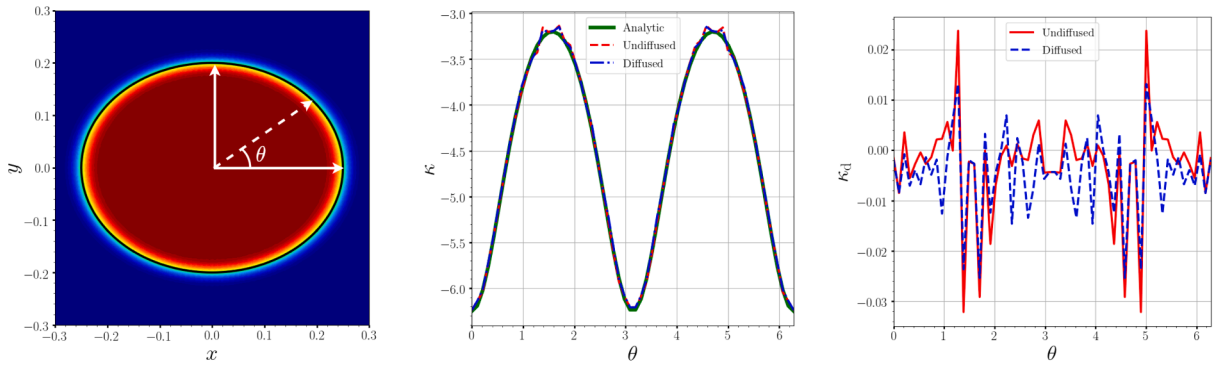

(a) Ellipse $(x/a)^2 + (y/b)^2 = 1$ (b) Curvature κ (c) Curvature relative error κ_d

Fig. 2. Curvature of an ellipse computed using undiffused and diffused approaches as a function of θ. Here $h = 1/100$, $D = 0.1h$, $\Delta\tau = 0.1h$ with 3 iterations performed. Note the domain size for this case is $\Omega = [-1, 1] \times [-1, 1]$ and the conservative let-set function is shown in (a).

3. Test problem 1: reversible vortex

In this benchmark problem, the signed distance function

$$\Phi_0(\mathbf{x}) = \sqrt{(x - 0.5)^2 + (y - 0.75)^2} - 0.15 \tag{6}$$

is initialised on the domain $\Omega = [0, 1] \times [0, 1]$. The initial configuration is a circle with centre $\mathbf{x} = (0.5, 0.75)$ and radius $r = 0.15$. The velocity field imposed on the level-set equations is derived from the stream function

$$\Psi(\mathbf{x}, t) = -\frac{1}{\pi} \sin^2(\pi x) \sin^2(\pi y) \cos\left(\frac{\pi t}{T}\right). \tag{7}$$

Mesh resolutions $h = 1/64, 1/128, 1/256$ and $1/512$ are considered on a structured mesh with a CFL number of unity on all meshes. The final time of the simulation is $T = 8$ with reversal occurring at $t = T/2$. The interface thickness was chosen to be $\epsilon = \frac{5}{8}h$ and the reinitialisation pseudo time step is $\Delta\tau = 0.1h$. The reinitialisation equation is solved until the change within each pseudo-time step less than 1 %. This process occurs once every 9 standard time iterations. In the traditional level-set method the scaling parameters for the calculation of the sign function are chosen to be $\epsilon_1 = h$ and $\alpha = 0.00625h$. Predictions made by the non-CLSM (NCLSM) and CLSM with and without reinitialisation are considered together with the proposed diffusion with the CLSM. The reinitialisation equation used in the NCLSM is

$$\frac{\partial \phi}{\partial \tau} + S(\phi_0)(1 - |\nabla \phi|) = \alpha \nabla^2 \phi \tag{8}$$

where ϕ is a signed distance function, $S(\phi_0)$ is a discrete approximation to the sign function and α is a diffusion parameter used to stabilise the nonlinear equation. In the CLSM, the reinitialisation equation (4) is employed instead, where the interface normal is determined using the current value of the level set function. In the diffused CLSM, the reinitialisation equation is the same but $\mathbf{n}$ is found using the diffused level set function calculated using (5). For more information on the reinitialisation equations used, please see [1] for the NCLSM, Eq (8) in [2] for the CLSM and Section 2.3 in [6] for the diffused CLSM. For quantitative comparison, Table 1 shows the L^2 error calculated with respect to the initial and final interface position and the percentage mass variation for all cases, in which CLSM has much better mass conservation compared to NCLSM.

In order to compare the CLSM qualitatively the position of the interfaces is visualised in Fig. 3 for the whole conservative level-set function at $t = 4$ and $t = 8$ for the mesh resolution $h = 1/512$. Fig. 3(a) shows the base CLSM without reinitialisation or diffusion. Here, much as for the non-reinitialised NCLSM, the level-set function begins to lose the continuous Heaviside properties it had initially. The smearing especially for the final profile at $t = 8$ results in a highly inaccurate interfacial region which in practice would completely ruin the hydrodynamics in a two-phase flow problem although the prediction of the 0.5 level-set is good.

In order to improve the retention of the properties associated with a smeared Heaviside function, reinitialisation is performed for Fig. 3(b). Here the properties are retained significantly better, resulting in a final profile with no smearing of the interface. The drawback is a slightly less accurate approximation of the interface. At the time of reversal $t = 4$, the tail begins to fragment as the reinitialisation struggles to resolve areas where the conservative level-set function changes rapidly from 0 to 1 and then to 0 again. Additionally, at final time $t = 8$, the final profile is much less like a perfect circle visually due to the sharp edges over the interface.

Finally, Fig. 3(c) shows how the resolution of the level-set function changes when the diffusive step is included in the algorithm. This process is used in practice to diffuse the level-set function for simpler normal calculation on fine interface resolutions. The main difference when compared to Fig. 3(b) is a small increase in fragmentation at the tail as a result of the diffused normal being used and an improvement in the circular topology of the final interface profile. Table 1 also illustrates how the addition of a diffusion step has little effect on the local or global mass conservation properties of the scheme, but a significant effect on the resolution of the interface. This makes it a useful addition to an interface representation algorithm which tends to have problems with particularly fine resolutions of the interface.

Table 1
Mass variation for the non conservative and conservative level-set methods. 'R' indicates reinitialisation and 'D' indicates diffusion.

		1/64	1/128	1/256	1/512
NCLSM	L^2 error	7.08×10^{-3}	2.99×10^{-3}	1.60×10^{-3}	7.15×10^{-4}
	Mass %	6.06 %	2.61 %	1.53 %	0.62 %
NCLSM + R	L^2 error	1.58×10^{-2}	1.02×10^{-2}	6.23×10^{-3}	1.49×10^{-3}
	Mass %	19.4 %	5.56 %	3.47 %	0.75%
CLSM	L^2 error	3.54×10^{-3}	1.52×10^{-3}	8.39×10^{-4}	4.69×10^{-4}
	Mass %	0.7 %	0.15 %	0.09 %	0.02%
CLSM + R	L^2 error	8.30×10^{-3}	2.80×10^{-3}	1.19×10^{-3}	9.28×10^{-4}
	Mass %	3.85 %	0.15 %	0.12 %	0.03%
CLSM + D + R	L^2 error	8.30×10^{-3}	2.10×10^{-3}	1.28×10^{-3}	1.09×10^{-3}
	Mass %	2.09 %	0.15 %	0.11 %	0.03%

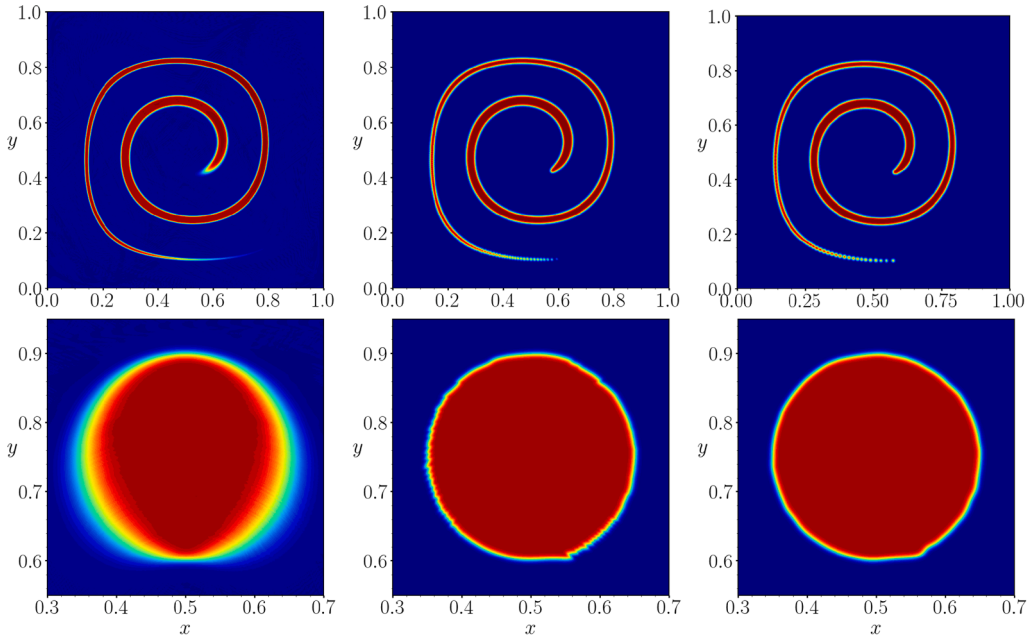

Fig. 3. Comparison between the normal conservative level-set method (a), the CLSM with reinitialisation (b) and the CLSM with diffusion and reinitialisation (c). Top panel displays the vortex at $t = 4$ at its most deformed state while bottom panel shows its structure at $t = 8$ after reversal.

4. Test problem 2: oscillating droplet

In order to validate the diffused interface approach for flows in which surface tension is the primary source of motion, the case of an oscillating droplet in 2D was considered. We consider both the approximate analytical solution (see [10]) to the problem and another numerical prediction from the literature (see [11]). The same computational setup of [11] is used with a square domain with side lengths $L = 0.075$ m and an initially ellipsoidal droplet with $r_{\text{avg}} = 0.02256$ m. Three mesh resolutions were considered ranging from $h = L/64$ to $h = L/256$, in order to demonstrate mesh convergence. The relevant material parameters are $\rho_1 = 787.88$ kg/m^3, $\mu_1 = 2.4 \times 10^{-2}$ Pa s, $\rho_2 = 1.1768$ kg/m^3, $\mu_2 = 2 \times 10^{-3}$ Pa s. There is no gravity and $\sigma = 0.02361$ N/m. The evolution of the y component of the north pole of the droplet is shown in Fig. 4. As can be seen we have good agreement with the period of oscillation. The amplitude can also be seen to be converging with mesh refinement. Lamb [10] provides an approximate analytical solution to the period shown in Table 2. Our values are also presented for each mesh and are in good agreement with the analytical value for validation of the test case.

Table 2
Comparison of the approximate analytical and computed periods of oscillation.

Analytical	64 × 64	128 × 128	256 × 256
1.5888	1.5577	1.5501	1.5547

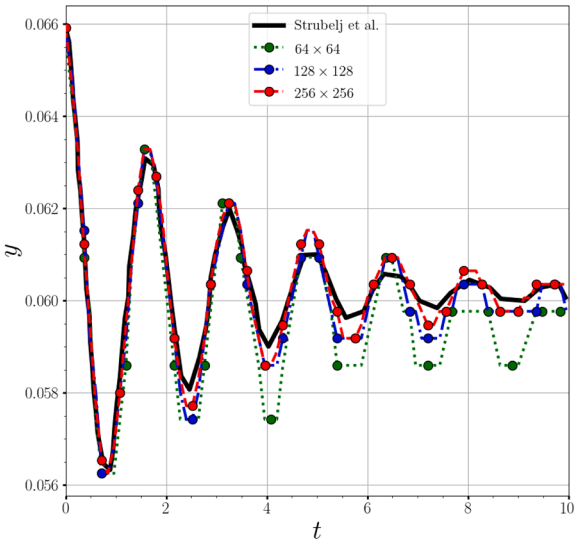

Fig. 4. Comparison of the evolution of the north pole interface position for an initially ellipsoidal droplet on mesh size and the simulations of Strubelj et al. [11]. Here $\epsilon = \frac{5}{8}h$, $D = 0.5h$ and $d\tau = 0.5h$ with 1 diffusion iteration.

5. Test problem 3: bubble rising in a viscoelastic fluid

In this problem a bubble rises along the centreline of a cylinder containing viscoelastic fluid. Axisymmetric flow is assumed. The experimental results are for 0.8 wt.% Praestol 2500 [12]. There is a critical bubble volume at which a jump in the terminal rise velocity is observed [12] and predicted numerically [6]. The value of the diffusion coefficient has been reported to have a negligible effect on the evolution of the bubble rise velocity and the variation in bubble volume [6].

Fig. 5a–d compares the profiles for a super-critical bubble with $V = 70$ mm^3 once a terminal rise velocity has been attained for the CLSM without diffusion (Fig. 5a), stabilized CLSM (SCLSM) (Fig. 5b), CLSM with $D = 0.1h$ applied to just the curvature calculation (Fig. 5c) and CLSM which additionally uses reinitialisation (Fig. 5d). The primary difference between the SCLSM in Fig. 5b and no diffusion in Fig. 5a is a replacement of the fragmentation of the cusp with a smeared profile instead. The mitigation of these dynamics is generally desired since they are not predicted by either experimental or numerical studies [12,13] and are a numerical artefact associated with the base CLSM, which produced a smeared interface. While providing an improvement over the simple L^2 projection, the SCLSM does not remove the smearing of the level set function in the wake region entirely and thus further fragmentation at the cusp could occur for bubbles of a larger volume or those represented with a more shear-thinning model. In Fig. 5c the diffused interface approach is applied purely to the curvature calculation and not the reinitialisation equation, resulting in a profile slightly improved from Fig. 5a as much of the fragmentation has been replaced with smearing dynamics. In Fig. 5d the interface is diffused according to the diffused interface approach with $D = 0.1h$ for all normal vectors used (reinitialisation and curvature), resulting in a cusp which is neither fragmented nor smeared but which retains the sharpness found experimentally.

The nature of the shape of the bubble near the trailing edge can be controlled by varying the value of D. This is shown in Fig. 5(e)–(i) in which 3D isosurfaces of the bubble are presented. In Fig. 5(g) and (i) the predictions made by the numerical scheme for the surface of the bubble with diffusion coefficients $D = 0.05h$ and $D = 0.2h$ are given. A reduction in the diffusion coefficient contributes to a sharper cusp, similar to those predicted by the SCLS and undiffused methods shown in Fig. 5(f) and (e), respectively. As $D \to 0$ the level set function becomes progressively less diffused, increasing the likelihood of undesirable fragmentation. On the other hand as D is increased, the shape of the trailing edge becomes more concave as the level set function used for the normal calculation is less sharp. Our investigations have shown that the optimal implementation of the diffused interface approach is achieved when the interface is diffused over one to three iterations with a time step and diffusion coefficient equivalent to 10 % of the spatial resolution, which ensures that there is just enough diffusion to avoid unphysical fragmentation or smearing, while retaining the sharp cusp at the trailing edge.

6. Test problem 4: droplet impact in a deep pool

The test problem of a droplet impacting a deep pool is considered here to assess the suitability of the diffused interface approach for a test problem involving coalescence and break-up dynamics. An axisymmetric droplet of diameter $d = 1.8$ mm is created at $x = (0, 11.4)$ mm in the domain $\Omega = [0, 20] \times [0, 20]$ mm. At $y_c = 10$ mm the interface between the surrounding air and the fluid is created. The fluid contained within the droplet and the deep pool is the same and Newtonian. The fluid considered is the 5 cSt silicone

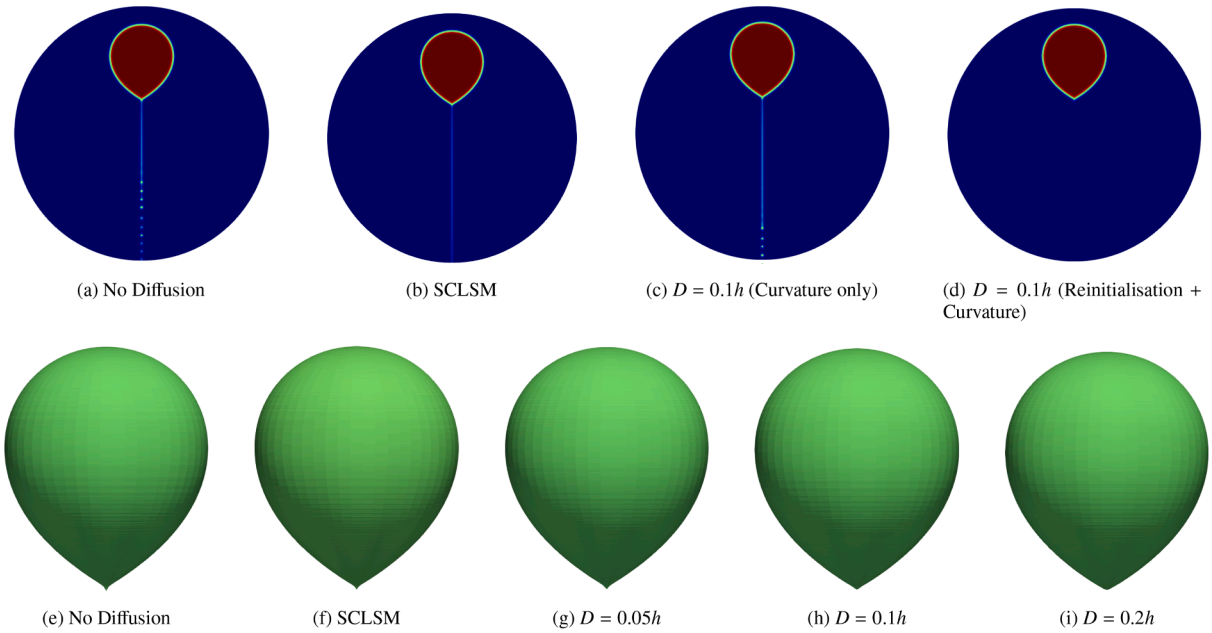

Fig. 5. Viscoelastic rising bubble of volume $V = 70$ mm^3. Comparison between the SCLSM and CLSM with different values of choice of diffusion coefficient D for the (a)-(d) 2D level-set function and (e)-(i) 3D isosurface.

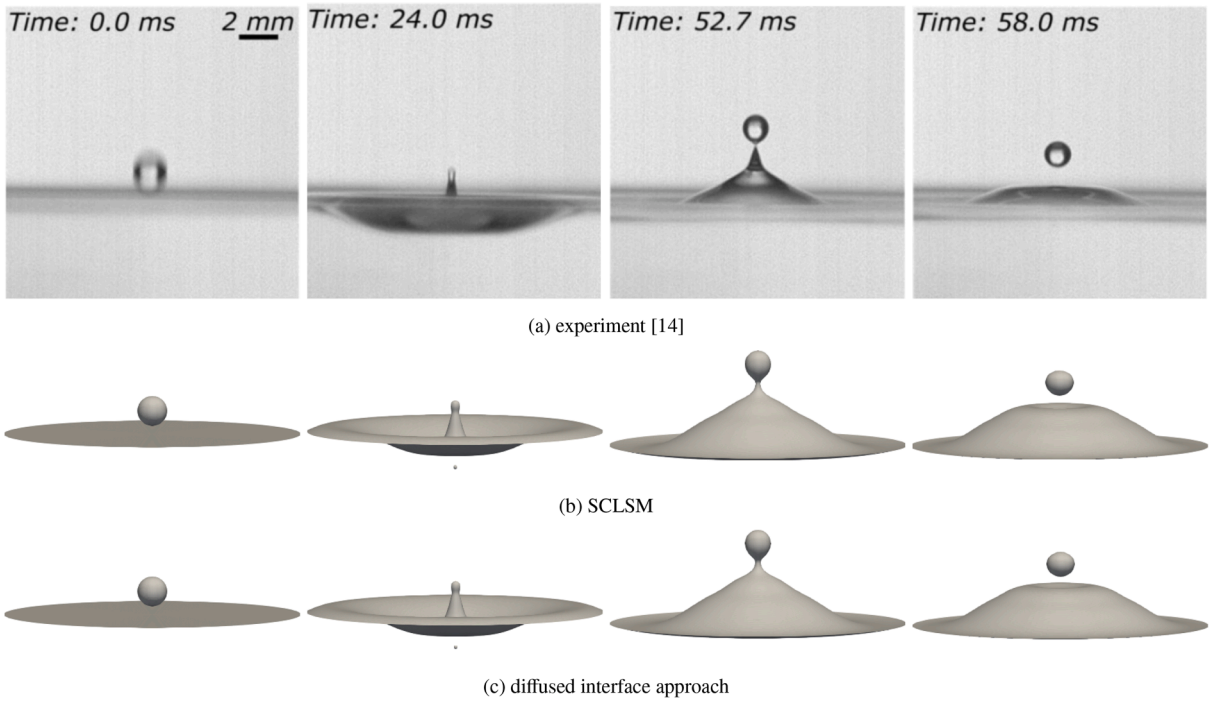

Fig. 6. Comparison of the numerical predictions of the bubble interface with experimental results [14] for different times.

oil solution from Table 1 in [14]. The mesh resolution used here is $h \approx 5.5$ μm compared to [14] who use $h \approx 5$ μm. Simulations are performed until dimensional time $T = 58$ ms with a time-step of $\Delta t = 2.5 \times 10^{-6}$ ms.

For the diffused interface approach, we use a diffusion parameter $D = 0.1h$ with a pseudo-time step of $\Delta\tau = 0.1h$ for one iteration. We compare the results obtained using the diffused interface approach with the experimental results and the SCLS method of [7]. In Fig. 6 the results are compared for times $t = 0$, 24, 52.7 and 58 ms, in which the present results show excellent agreement across all time steps with the experimental work. The main difference is at $t = 52.7$ ms where the diffused interface approach predicts a

(a) SCLSM (b) Diffused interface (c) More diffusion

Fig. 7. Comparison of the SCLSM and the diffused interface method with different diffusion at $t = 54$ ms.

slightly broader liquid bridge connecting the droplet to the collapsing jet structure. This is further investigated in Fig. 7 at $t = 54$ ms, at which there is no experimental snapshot to compare with, but the simulations predict the point immediately before separation. We compare the method of [7] with the diffused interface approach using 1 and 3 iterations. It can be seen that more diffusion results in a broader liquid bridge with no other discernible effect on the droplet and jet structure. The diffused interface approach is shown here to capture the dynamics of break-up and coalescence well while stabilizing the normal projection step.

7. Summary

In this contribution, we propose a diffused interface approach for the conservative let set method, which results in better interface normal and curvature calculations. The additional diffusion step not only keeps the interface sharp and mass conserved as the original CLSM during interface capturing, but also provides accurate surface tension calculation which plays a crucial role in both Newtonian and non-Newtonian [6] multiphase flow simulations.

CRediT authorship contribution statement

William Doherty: Writing – original draft, Visualization, Validation, Software, Methodology, Investigation, Formal analysis, Data curation; **Timothy N. Phillips:** Writing – review & editing, Writing – original draft, Supervision, Methodology, Investigation, Formal analysis, Conceptualization; **Markus Uhlmann:** Writing – review & editing, Validation, Resources, Investigation, Formal analysis; **Zhihua Xie:** Writing – review & editing, Writing – original draft, Supervision, Methodology, Investigation, Funding acquisition, Formal analysis, Conceptualization.

Data availability

Data will be made available on request.

Declaration of competing interest

The authors declare that they have no known competing financial interests or personal relationships that could have appeared to influence the work reported in this paper.

Acknowledgments

Constructive comments from two anonymous reviewers and the Associate Editor have helped to improve the manuscript and these are gratefully acknowledged. This work is supported by EPSRC grants (EP/R513003/1 with studentship reference 2397637 and EP/V040235/1). ZX is partially supported by the Alexander von Humboldt Research Fellowship for experienced researchers in Germany.

References

[1] S. Osher, J.A. Sethian, Fronts propagating with curvature-dependent speed: algorithms based on Hamilton-Jacobi formulations, J. Comput. Phys. 79 (1) (1988) 12–49.
[2] E. Olsson, G. Kreiss, S. Zahedi, A conservative level set method for two phase flow II, J. Comput. Phys. 225 (1) (2007) 785–807.
[3] Z. Xie, D. Pavlidis, P. Salinas, J.R. Percival, C.C. Pain, O.K. Matar, A balanced-force control volume finite element method for interfacial flows with surface tension using adaptive anisotropic unstructured meshes, Comput. Fluids 138 (2016) 38–50.
[4] P. Yue, C. Zhou, J.J. Feng, Sharp-interface limit of the Cahn-Hilliard model for moving contact lines, J. Fluid Mech. 645 (2010) 279–294.
[5] M.M. Francois, S.J. Cummins, E.D. Dendy, D.B. Kothe, J.M. Sicilian, M.W. Williams, A balanced-force algorithm for continuous and sharp interfacial surface tension models within a volume tracking framework, J. Comput. Phys. 213 (1) (2006) 141–173.
[6] W. Doherty, T.N. Phillips, Z. Xie, The log-conformation formulation for single- and multi-phase axisymmetric viscoelastic flows, J. Comput. Phys. 508 (2024) 113014.
[7] N. Shervani-Tabar, O.V. Vasilyev, Stabilized conservative level set method, J. Comput. Phys. 375 (2018) 1033–1044.
[8] W. Doherty, T.N. Phillips, Z. Xie, A stabilised finite element framework for viscoelastic multiphase flows using a conservative level-set method, J. Comput. Phys. 477 (2023) 111936.

[9] N.A. Ilangakoon, A.G. Malan, B.W.S. Jones, A higher-order accurate surface tension modelling volume-of-fluid scheme for 2D curvilinear meshes, J. Comput. Phys. 420 (2020) 109717.
[10] H. Lamb, Hydrodynamics, The University Press, Cambridge, U.K., Cambridge, U.K., 1924.
[11] L. Štrubelj, I. Tiselj, B. Mavko, Simulations of free surface flows with implementation of surface tension and interface sharpening in the two-fluid model, Int. J. Heat Fluid Flow 30 (4) (2009) 741–750.
[12] C. Pilz, G. Brenn, On the critical bubble volume at the rise velocity jump discontinuity in viscoelastic liquids, J. Nonnewton. Fluid Mech. 145 (2-3) (2007) 124–138.
[13] D. Fraggedakis, M. Pavlidis, Y. Dimakopoulos, J. Tsamopoulos, On the velocity discontinuity at a critical volume of a bubble rising in a viscoelastic fluid, J. Fluid Mech. 789 (2016) 310–346.
[14] E. Castillo-Orozco, A. Davanlou, P.K. Choudhury, R. Kumar, Droplet impact on deep liquid pools: Rayleigh jet to formation of secondary droplets, Phys. Rev. E 92 (2015) 053022.